polymer communications

Brillouin spectroscopy of oriented PMMA

J. K. Krüger
Universität des Saarlandes, Fachrichtung 11.2 – Experimentalphysik, 66 Saarbrücken, West Germany

and M. Pietralla
Universität Ulm, Abteilung für Experimentalphysik, 79 Ulm, West Germany
(Received 27 April 1981; revised 2 July 1981)

The elastic properties of oriented PMMA have been re-investigated by Brillouin spectroscopy. Most of the elastic stiffness tensor components are presented. The order parameter P_2 has been determined as a function of orientation and is compared with P_2 deduced from other methods. Previously reported elastic anomalies of oriented PMMA[7a,b] could not be confirmed

Keywords Spectroscopy; Brillouin; poly(methyl methacrylate); orientation; elastic properties; order parameter

Introduction

Since the orientation of molecules within a polymer widely affects the elastic properties, it seems in turn useful to take the elastic properties to characterize the orientational state of polymers. However, for this purpose, in general a complete knowledge of the elastic tensor is required which is usually difficult to obtain[1]. Modern Brillouin spectroscopy (BS) offers an elegant and relatively simple method of obtaining the complete elastic tensors of polymers with a minimum of constraints regarding the shape and the transparency of the samples[2–6]. Lindsay *et al.*[7a,b] were the first to have published such measurements of oriented PMMA which led to an unexpected result: In contrast to ultrasonics[8] where the sound velocity in the draw direction increases with drawing, it remained constant at the value of the isotropic material in the hypersound region. Only the sound velocity perpendicular to the draw direction was affected by the drawing process. In addition Lindsay *et al.* observed hypersonic dispersion. Since these findings do not conform to our results on biaxially oriented PA-6-3T[2] we reinvestigated several uniaxially oriented PMMA samples taking advantage of a special scattering geometry[3,5]. As a result we can present most of the elastic tensor components. The orientation parameter determined will be compared with results of other methods.

In contradiction to the findings of Lindsay *et al.*[7] the hypersound velocity in the draw direction increases with the orientation. No hypersonic dispersion has been observed and the Rayleigh peak intensity was not indicative for exceeding void formation with orientation.

Experimental

For the determination of the elastic properties of the oriented PMMA samples we used Multipass-BS. The spectrometer has been described elsewhere[9]. The free spectral range was set to 11.9 GHz for optimum frequency resolution. The finesse of the Fabry Perot was about 45.

The four samples were commercial PMMA (Plexiglas® 233) with viscosimetric molecular weight $M_w = 5.10^6$. They were stretched above the glass temperature and samples a, c, d were quenched with liquid nitrogen. Sample b was slowly cooled to room temperature. From the orientated samples, pieces of length ~20 mm were cut and mounted into a goniometer enabling rotation around the y-axis of the sample in the 90 A scattering geometry (cf. *Figure 1*)[5,9]. Using this scattering geometry the phonon wave vector $\vec{q}$ remains in the xz-plane of the sample moreover for the VV-scattering arrangement the value of

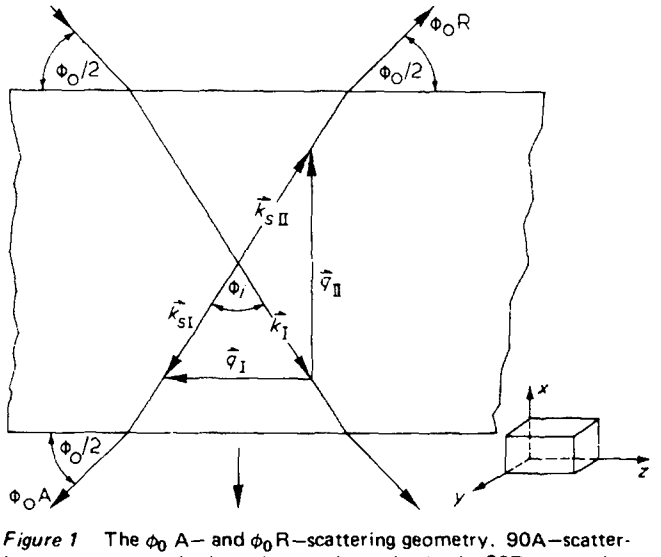

Figure 1 The ϕ_0 A– and ϕ_0R–scattering geometry. 90A–scattering geometry: y-axis along the rotation axis. In the 90R–scattering geometry $\vec{q}$ points along the y-axis. Only the xz-surfaces must be of optical quality. $\vec{k}_i$ wave vector of the incident laser light, $\vec{k}_{sI}$ and $\vec{k}_{sII}$ wave vector of the scattered light in the ϕ_0A– and ϕ_0R–scattering geometry respectively. $\vec{q}_I$ and $\vec{q}_{II}$ the corresponding phonon wave vectors

q remains constant.

$$\Lambda = \frac{\lambda}{2n_0 \sin\frac{\varphi_0}{2}} \quad (1)$$

with

$$n_0 \sin\frac{\varphi_0}{2} = n_i^{i,s} \sin\frac{\varphi_i}{2} \quad \text{(Snellsius law)}$$

and $\Lambda = 345{,}07$ nm acoustic wave length; $\lambda = 488$ nm optical wave length; $n_0 = 1$ outer refractive index, $n_i^i = n_i^s$ refractive index for the incident (i) and scattered (s) light; $\varphi_0 = 90°$ outer scattering angle; φ_i inner scattering angle.

If $n_i^i = n_i^s$, this constancy of the phonon wave length holds even for cases where the polarization vector of the incident and scattered light are not directed along the principal axis of the optical indicatrix. Therefore all the sound velocities given in *Figures 2* and *3* do not contain the usual uncertainity of the refractive index and are all measured for the same acoustic wave length $\Lambda = 345.07$ nm. The absolute accuracy of our sound velocity data and elastic stiffness constant are about 1%. Within an accuracy of about 3%, the phonon linewidth remained constant as a function of sample orientation. The Rayleigh peak intensity was not affected by the drawing process, indicating that no serious increase of voids took place. In the literature reported, additional weak phonons [7b] were also not observed.

The birefringence was measured at the scattering volume using a polarization microscope (Leitz Orthoplan-Pol) with a tilting compensator (Leitz 997M).

Results and Discussion

A plot of the sound velocity *versus* orientation angle θ for the samples a and d is shown in *Figure 2*. The elastic stiffness components follow from the Christoffel equation[10]:

$$\left[\underset{\sim}{A} - \underset{\sim}{E}\left(\frac{\rho\omega^2}{q^2}\right)\right]\vec{u} = 0 \quad (1)$$

where $\vec{u}$ is the particle displacement, $\omega/2\pi$ the sound frequency, q the value of the wave vector, ρ the density, $\underset{\sim}{E}$ the unit matrix and $\omega/q = v$ is the sound velocity. For fibre symmetry with respect to the draw direction (z-axis, $\theta = 0$) and with q in the xz-plane (*Figure 1*) the non-vanishing elements of $\underset{\sim}{A}$ are

$$A_{11} = c_{11}l_x^2 + c_{44}l_z^2 \quad A_{13} = A_{31} = (c_{13} + c_{44})l_x l_z$$
$$A_{22} = c_{66}l_x^2 + c_{44}l_z^2 \quad l_x = \sin\theta,\ l_z = \cos\theta$$
$$A_{33} = c_{44}l_x^2 + c_{33}l_z^2 \quad c_{ij} \text{ are the elastic stiffness components in the Voigt notation.}$$

$$\theta = \sphericalangle(\vec{q}, z\text{-axis})$$

The solving of the eigenvalue problem posed by equation (1) leads us to the following relations between the measured quantities v, ρ, θ and the unknown elastic stiffness components:

$$v_{QL/QT}(\theta) = (2\rho)^{1/2}\{c_{11}\sin^2\theta + c_{33}\cos^2\theta + c_{44(\pm)}K\}^{1/2} \quad (2a)$$

where

$$K = \{[c_{11} - c_{44})\sin^2\theta + (c_{44} - c_{33})\cos^2\theta]^2 + (c_{13} + c_{44})^2\sin^2 2\theta\}^{1/2} \quad (2b)$$

On account of the small scattering cross-section of the quasi-transverse phonons v_{QT} was not measured.

By performing a least squares fit with equations 2a and 2b to the experimental $v_{QL}(\theta)$-curves the elastic stiffness constants were calculated (*Table 1*). The resulting fit curves of samples a and d are also shown in *Figure 2*. In *Figure 3* a polar plot $v_{QL}(\theta)$ of sample d is shown.

Whether the assumption of fibre symmetry was correct or not was tested in the following way for sample d: Using the 90N-scattering geometry[3] with the VV-arrangement the frequency of phonons with wave vector $\vec{q}$ bisecting the zy-angle were measured. Furthermore the 90R-scattering

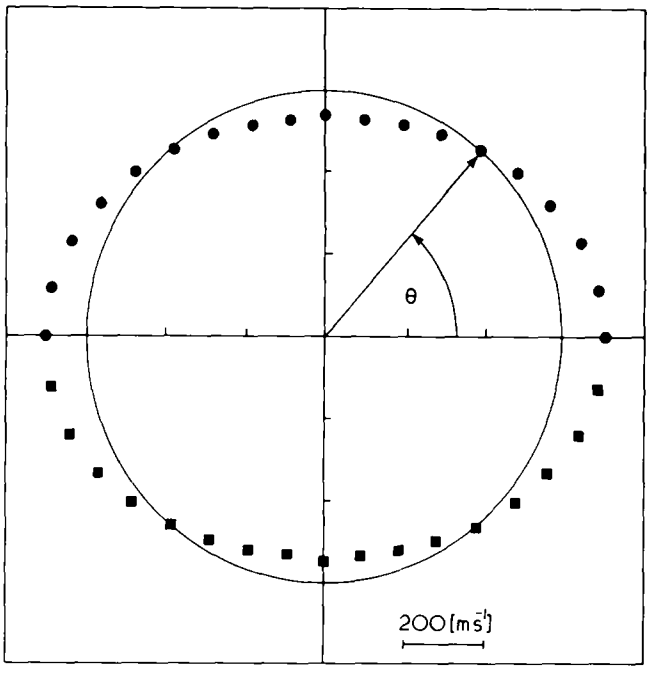

Figure 3 Polar plot of the sound velocity of sample d where the scale includes a zero point suppression of 2 km s^{-1}. The large circle represents the sound velocity of the isotropic sample. ●, Data points of sample d; ■, are points derived from ● by symmetry

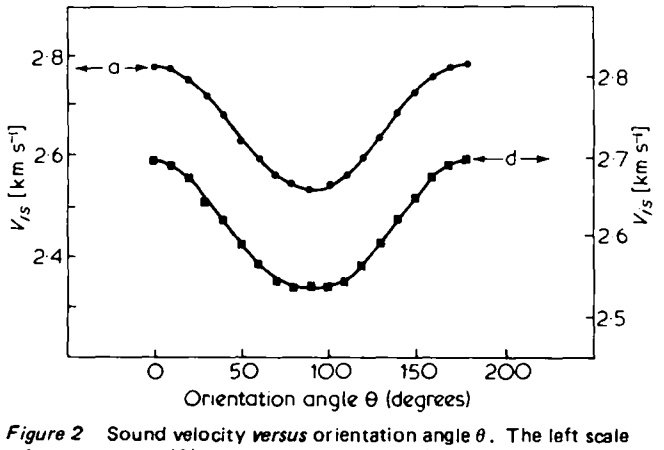

Figure 2 Sound velocity *versus* orientation angle θ. The left scale refers to sample a(●), the right to sample d(■). The sound velocity of the isotropic PMMA samples is $v_{/S}$ = 2.6 km s^{-1}

Table 1

Sample	c_{11}: [GPa]	c_{33}: [CPa]	c_{44}: [GPa]	c_{13}: [GPa]	c_{11}^{iso}: [GPa]	$(c_{33}-c_{11})/c_{11}$	$-\Delta n.10^4$	P_2
a	7.63	9.16	3.67	1.0	8.02	0.20	9.17	0.13
b	7.85	8.32	3.43	1.09	8.01	0.6	3.78	0.04
c	7.66	8.89	–	–	8.01	0.16	8.04	0.10
d	7.66	8.68	3.36	1.28	8.02	0.13	8.30	0.08

a, b, c, d temperature of drawing 110 ± 2°C, speed of drawing $\lambda = 5.4\ 10^{-3}\ s^{-1}$, temperature of elastic and optic measurements 23°C

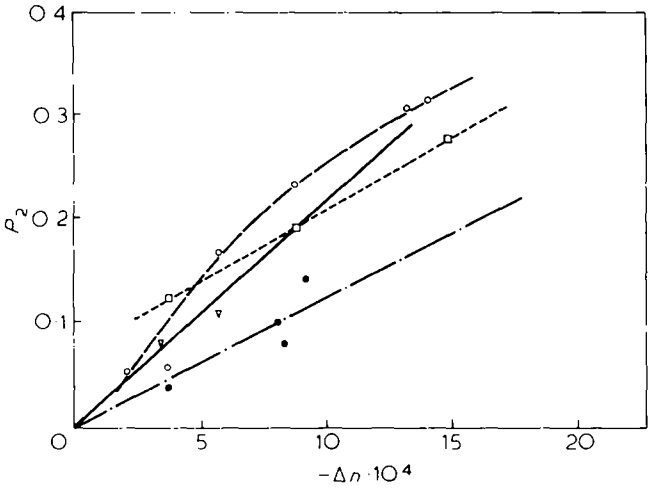

Figure 4 The orientation parameters P_2 *versus* birefringence: ○, From n.m.r.[12]; □, from Raman scattering[11]; △, from X-ray scattering[15] and ●, from BS scattering

geometry[3] was used to measure the frequency of phonons travelling along the y-axis where the optical polarization was parallel to the z-axis. In the case of fibre symmetry both the measurements lead directly to c_{11} already determined by the 90A-scattering geometry.

$$90N: c_{11} = \rho\{f_N \lambda_\omega / 2n_z \sin(\pi/4)\}^2 \quad (3)$$

$$90R: c_{11} = \rho\{f_R \lambda_\omega / 2n_z \sin(\varphi/2)\}^2 \quad (4)$$

$$90A: c_{11} = \rho\{f_A \lambda_\omega / 2\sin(\pi/4)\}^2 \quad (5)$$

$$\text{where } \sin(\varphi/2) = \cos\{\arcsin[\sin(\pi/4)/n_z]\} \quad (4a)$$

n_z is the refractive index for polarization along the z-axis, $f_{N,R,A}$ are the sound frequencies measured in the geometry given by the index, λ_ω is the vacuum laser wave length. The values used are $\lambda_\omega = 488$ nm, $f_N = 11.90$ GHz, $f_R = 13.83$ GHz, $f_A = 7.35$ GHz.

On account of the constant phonon linewidths for the different wave vectors significant accoustic dispersion could be excluded. Hence from the 90N (3) and 90A (5) arrangements the refractive index n_z (488 nm) = 1.509 could be determined from the measured Brillouin frequency shifts. This refractive index was then used in equation (4): The constant c_{11} computed in this way had only a deviation of 0.2% from that determined directly in the 90A-arrangement. Thus the assumption of the fibre symmetry is fully justified.

In contrast to the investigations of Lindsay *et al.*[7] the inequality $c_{11} < c_{11}^{iso} < c_{33}$ holds for all the samples. It is not yet clear where this discord comes from: Lindsay *et al.* explained their results in terms of void formation and local densification. A striking feature is that this compensates just for the increase of the elastic stiffness which occurs in the draw direction (see *Table 1* and *Figure 4*). As was pointed out above we had no indication for such densification and void formation in our samples although two of our samples showed a comparable double refraction ($n = -4.10^{-4}$ and -9.10^{-4}) and the preparation conditions seem to be similar (drawing at 120–130 C). Lindsay *et al.* relate the additional phonon which they found in their spectra to rarified regions ('phase separation'). From our experiences with 'phase separations'[3,4,16] we do not believe in this explanation, because neither the Rayleigh intensity nor the sound attenuation correspond to our observations in polymers with macroscopic (compared with the acoustic wave length) regions of different acoustic impedance.

Following Moseley[11] and Stein[12] the average molecular orientation can be characterized by the orientation parameter

$$P_2 = \langle P_2(\cos\theta)\rangle = (3\langle\cos^2\theta\rangle - 1)/2 = 1 - v_{is}^2/v_z^2 \quad (6)$$

where v_z is the sound velocity in the draw direction and v_{is} that of the isotropic sample. The values of P_2 are given in *Table 1*.

It is interesting to compare the orientation parameter P_2 determined in this way with values determined by other methods. For this purpose we plot P_2 against the birefringence which itself should be proportional to this parameter according to

$$\Delta n = \Delta n_0 P_2 \quad (7)$$

where Δn_0 is the intrinsic birefringence usually attributed to monomer units.

Plots of P_2 *versus* Δn determined by different methods are shown in *Figure 4*. Whereas P_2 derived from BS-measurements and that from X-ray scattering data[15] exhibit a proportionality according to equation (7), the values derived from Raman[13] and from n.m.r.[14] measurements do not. The corresponding intrinsic birefringence is $\Delta n_0 = -67 \times 10^{-4}$ (BS) and -47×10^{-4} (X-ray). The differences in P_2 determined by the various methods may be due to two contributions:

(i) The numerous assumptions needed for the evaluation of P_2 from the measured physical properties[16].

(ii) The fact that the real structural units operative in each physical effect, including birefringence, are different on account of interaction effects beyond orientational superposition.

On the macroscopic scale the state of order is favourably described by the elastic tensor because it is of fourth rank. BS-measurements offer the most efficient way to determine this tensor. The dependence of this tensor on the molecular orientation of non-crystalline polymers is however not fully understood. To overcome the apparent discrepancies we need the knowledge of the proper (structural) order parameter and its coupling to the measured physical properties.

Acknowledgement

The authors are indebted to H. R. Schubach for his help with the sample preparation. The authors acknowledge fruitful discussions with Prof Dr H.-G. Unruh. This work was kindly supported by the Deutsche Forschungsgemeinschaft.

References

1 Ward, I. M. 'Structure and Properties of Oriented Polymers', Applied Science Publishers Ltd., London, 1975
2 Krüger, J. K., Sailer, E., Spiegel, R. and Unruh, H.-G. *Progr. Colloid Polym. Sci.* 1978, **64**, 208
3 Krüger, J. K., Peetz, L. and Pietralla, M. *Polymer* 1978, **19**, 1397
4 Krüger, J. K., Marx, A. and Peetz, L. *Ferroelectrics* 1980, **26**, 753
5 Krüger, J. K., Bastian, H., Asbach, G. I. and Pietralla, M. *Polym. Bull.* 1980, **3**, 633
6 Sandercock, J., Festkörperprobleme (Ed. H. J. Quisser), 1975, XV, 183 (Pergamon, Braunschweig)
7a Lindsay, S. M., Hartley, A. H. and Shephard, I. W. *Polymer* 1976, **17**, 501
7b Lindsay, S. M. and Shephard, I. W. *J. Polym. Sci.: Polym. Symp.* 1977, **58**, 85
8 Wright, H., Faraday, C. S. N., White, E. F. T. and Treloar, L. R. G. *J. Phys. D. Appl. Phys.* 1971, **4**, 2002
9 Krüger, J. K., Peetz, L., Pietralla, M. and Wildner, W. *Polymer* 1980, **21**, 620
10 Auld, B. A. 'Acoustic Fields and Waves in Solids', Vol 1, J. Wiley, London, 1973
11 Moseley, W. W. Jr., *J. Appl. Polym. Sci.* 1960, **3**, 266
12 Stein, R. S. in ref. 1, pp 133
13 Purvis, J. and Bower, D. I. *Polymer* 1974, **15**, 645
14 Kashiwagi, M., Folkes, M. J. and Ward, I. M. *Polymer* 1971, **12**, 697
15 Pick, M., Lovell, R. and Windle, A. N. *Polymer* 1980, **21**, 1017
16 Krüger, J. K., Peetz, L., Pietralla, M. and Unruh, H.-G. *Polym. Bull.* 1981, **4**, 591

Investigation of local viscosity in polymer solutions by means of electrolytic conductivity

Hans Vink
Institute of Physical Chemistry, University of Uppsala, P.O. Box 532, 751 21 *Uppsala, Sweden*
(*Received* 19 *May* 1981)

The local viscosity in aqueous solutions of polymers (dextran and hydroxyethyl cellulose) and low-molecular weight viscogenic compounds (glycerol and d-glucose) has been studied by measuring the electrolytic conductivity of probe electrolytes. For low-molecular weight viscogenic compounds the local viscosities determined were close to the macroscopic viscosities of the solutions, whereas pronounced differences exist for polymer solutions. Of particular interest was the finding that the local viscosity for dextran was only marginally higher than the local viscosity for the corresponding monomer, d-glucose. The local viscosity for hydroxyethyl cellulose was somewhat higher than the local viscosity for dextran, indicating greater flexibility of the dextran chain.

Keywords Polymer solutions; viscosity; conductance;dextran; glucose; hydroxyethyl cellulose; glycerol

Introduction

The local viscosity, or microviscosity, of a polymer solution can be studied by various diffusion methods, either by directly determining the diffusion coefficient of a probe molecule[1-4], or indirectly by fluorescence depolarization[5-7], diffusion determined reaction kinetics[8,9] and polarography[10,11]. In the present investigation an alternative method, based on the determination of the electrolytic conductivity of a probe electrolyte in polymer solutions, is used. This method is best suited to aqueous solutions and has certain advantages over the diffusion method. As the probes are subjected to a steady external force the method is directly related to Stokes' law, and does not involve Einstein's equation for the diffusion coefficient. The method also takes advantage of the simplicity and high inherent accuracy of conductivity measurements.

Theory

The limiting equivalent conductivity of a binary 1:1 electrolyte may be related to the frictional properties of the constituent ions by the equation

$$\Lambda^0 = \lambda_+^0 + \lambda_-^0 = \frac{F^2}{f_+} + \frac{F^2}{f_-} \qquad (1)$$

where Λ^0, λ_+^0 and λ_-^0 are the limiting equivalent conductivities of the electrolyte and the cation and anion, respectively, f_+ and f_- are the corresponding molar friction coefficients and F is the Faraday constant.

Using Stokes' law we may express the friction coefficients in the form

$$f_i = N_A 6\pi r_i \eta, \quad i = +, - \qquad (2)$$

where N_A is the Avogardro constant, r_i the ionic radius and η the local viscosity. It should be noted that in conjunction with the macroscopic viscosity, the constant factor 6π in equation (2) should be replaced by a smaller number (4π or smaller[12]) when applied to bodies of molecular dimensions. As the value of this factor is unknown, it is appropriate to retain the value 6π and define the (apparent) local viscosity by equation (2).

Combining equations (1) and (2) we obtain

$$\Lambda^0 = \frac{F^2}{N_A 6\pi\eta}\left(\frac{1}{r_+} + \frac{1}{r_-}\right) \qquad (3)$$

Thus, provided the ionic radii are constant, Λ^0 is a direct measure of the local solution viscosity. Denoting by Λ_0^0 and η_0 the values of the respective quantities in pure solvent (water) we have

0032 3861/82/010006 04$03.00